1   Manuscript for submission to *American Mineralogist*, REVISION #2-Mar 2018

2   Analysis and visualization of vanadium mineral

3   diversity and distribution

4   Chao Liu[1*], Ahmed Eleish[2], Grethe Hystad[3], Joshua J. Golden[4],

5   Robert T. Downs[4], Shaunna M. Morrison[4], Daniel R. Hummer[5], Jolyon P. Ralph[6],

6   Peter Fox[2] and Robert M. Hazen[1]

7

8   [1]*Geophysical Laboratory, Carnegie Institution for Science, 5251 Broad Branch Road NW, Washington, D.*
9   *C. 20015, USA.*
10   [2]*Tetherless World Constellation, Department of Earth and Environmental Sciences, Rensselaer Polytechnic*
11   *Institute, Troy NY 12180 USA*
12   [3]*Department of Mathematics, Computer Science, and Statistics,*
13   *Purdue University Northwest, Hammond, Indiana 46323, USA.*
14   [4]*Department of Geosciences, University of Arizona, 1040 East 4th Street, Tucson, Arizona 85721-0077,*
15   *USA.*
16   [5]*Department of Geology, Southern Illinois University, Carbondale, Illinois 62901, USA*
17   [6]*Mindat.org, 128 Mullards Close, Mitcham, Surrey, CR4 4FD, United Kingdom.*

18

19   **ABSTRACT**

20   We employ large mineralogical data resources to investigate the diversity and spatial

21   distribution of vanadium minerals. Data for 219 approved species (rruff.info/ima, as of 15

22   April 2016), representing 5437 mineral species-locality pairs (mindat.org and other

23   sources, as of 15 April 2016), facilitate statistical evaluation and network analysis of

24   these vanadium minerals. V minerals form a sparse, moderately centralized and transitive

25   network, and they cluster into at least 7 groups, each of which indicates distinct

26   paragenetic process. In addition, we construct the V mineral-locality bipartite network to

27   reveal mineral diversity at each locality. It shows that only a few V minerals occur at

28   more than 3 localities, while most minerals occur at 1 or 2 localities, conforming to a

29   Large Number of Rare Events (LNRE) distribution. We apply the LNRE model to predict

30   that at least 307 ± 30 (1σ) vanadium minerals exist in Earth's crust today, indicating that

31   at least 88 species have yet to be discovered—a minimum estimate because it assumes

32   that new minerals will be found only using the same methods as in the past. Numerous

33   additional vanadium minerals likely await discovery using micro-analytical methods. By

34   applying LNRE models to subsets of V minerals, we speculate that most new vanadium

35   minerals are to be discovered in sedimentary or hydrothermal non U-V ore deposits other

36   than igneous or metamorphic rocks/ore deposits.

37

38   **Keywords:** vanadium, network analysis, statistical mineralogy, LNRE frequency

39   distribution

_____

40

41   * E-mail: cliu@carnegiescience.edu

42

43

44

45

46

47

48

49

50

51   **INTRODUCTION**

52   The last century has seen the discovery of thousands of mineral species.

53 Characteristics of these mineral species, including their physical properties, chemical

54 compositions, and their localities of occurrence, have been parsed into large mineral

55 databases (e.g., rruff.info/ima and mindat.org). These mineralogical "big data" reveal

56 diversity and spatial distribution of all terrestrial minerals (Hazen et al. 2015a, 2015b,

57 2016a, 2016b; Hystad et al. 2015a, 2015b, 2016), facilitate network analysis of existing

58 minerals (Morrison et al., 2017), and lead to predictions of Earth's "missing" minerals

59 (Hazen et al. 2016a; Grew et al. 2016; Liu et al., 2016).

60   This study focuses on the diversity and spatial distribution of all terrestrial vanadium

61 (V) mineral species. V is a redox-sensitive first-row transition element of special interest

62 in geochemistry because it is an ideal oxygen fugacity tracer (Lee et al., 2003; Righter et

63 al., 2016), and might have played a major role in biological electron transfer early in

64 Earth's history (Rehder, 2008). In addition, it is of strategic importance (National

65 Research Council 2008; Orcutt 2011), environmental impact (Gummow, 2011), and

66 human-health significance (Mukherjee, 2004). V is a minor element in the crust,

67 averaging ~138 ppm in crustal abundance (Rudnick and Gao, 2005), with upper crustal

68 abundance of ~97 ppm (Rudnick and Gao, 2005) and lower crustal abundance of ~196

69 ppm (Rudnick and Fountain, 1995). V concentrations vary significantly among different

70 rock types. In igneous rocks, they range from ~40 ppm in ultramafic rocks, and ~60 ppm

71 in granitic rocks, to ~250 ppm in basaltic rocks (Mielke, 1979). In sedimentary rocks, the

72 average V content of quartzitic sandstone and pure carbonate sediments is <15 ppm, with

73 higher values in greywackes (40 to 150 ppm) and shales (90 to 260 ppm) (Koljonen,

74   1992). Most V is incorporated into rock-forming minerals as a trace element (e.g., Curtis,

75   1964; Huang et al., 2015), since V^{3+}, V^{4+} and V^{5+} readily substitute Fe^{3+}/Al^{3+}, Ti^{4+} and

76   P^{5+} in many common minerals. That being said, crystal chemical behavior of V cations is

77   not exactly the same as the substituted cations (e.g., Schindler and Hawthorne, 1999;

78   Schindler et al., 2000). For instance, V^{4+} and V^{5+} can develop one to two strong π-bonds

79   with oxygen forming either [3+2] or [4+1] coordination geometries, which allows VOx

80   polyhedra to polymerize to sheets and chains but does not allow their incorporation into a

81   3-dimensional network. Similarly, V^{3+} has electronic degeneracy that can drive

82   spontaneous distortions of its coordination polyhedra. Therefore, despite its extensive

83   substitution into common minerals as a trace element, the unique crystal chemistry of V

84   enables the formation of 219 minerals with V as an essential element (rruff.info/ima as of

85   15 April 2016; Downs 2006). This limited number of species makes it possible to

86   complete a comprehensive survey of vanadium mineral species and their localities.

87

88   **A SURVEY OF V MINERAL COMPOSITIONS**

89   Of the 72 essential chemical elements found in all mineral species (rruff.info/ima;

90   Hazen et al. 2015a), 44 are essential constituents of vanadium minerals (Table 3). The

91   most frequently encountered elements are oxygen (in 211 species) and hydrogen (147).

92   Next in abundance are common rock-forming elements Ca (51), Si (37), Al (31), Fe (30),

93   Na (29), Cu (28), Mn (26), Ba (20), and Pb (20). The remaining thirty-three elements are

94   each represented by fewer than 20 species. The number of essential elements in each V

95   mineral range from 1 (the mineral vanadium: V) to 9 (the mineral hanjiangite:

96    $Ba_2Ca(VAl)(AlSi_3O_{10})(OH)_2F(CO_3)_2$), with most species containing more than three

97   essential elements. Average chemical complexity, here defined as numbers of major

98   elements per formula, of all 219 V minerals is 4.6 elements per species, and the values

99   are similar among V^{3+} (5.1 elements per species), V^{4+} (4.4), and V^{5+} species (4.7).

100   However, different groups of elements are incorporated into V^{3+}, V^{4+}, and V^{5+} minerals.

101   Lithophile elements, including Si, Al, Ti, Ba, and B, are more likely present in V^{3+}

102   species, since V^{3+} has an ionic radius (78 pm), similar to Cr^{3+} (75.5 pm) and Fe^{3+} (69 pm;

103   78.5 pm, high spin), and is incorporated into octahedral sites in many rock-forming

104   minerals. Hydrogen, alkalis, alkaline earth elements, chlorine, UO^{2+} and divalent

105   transition elements (Mn, Cu, Pb, Zn) are found mostly in V^{5+} minerals, where they bind

106   with vanadate ion (VO_4^{3-}) to form sedimentary and hydrothermal minerals. Sulfur and

107   phosphorus are found mostly in V^{4+} species, in which vanadium is present as VO^{2+}, and

108   precipitate as sulfates and phosphates in sedimentary rocks.

109   Paragenesis of V minerals is closely related to V oxidation states. In general, V^{3+}

110   minerals are of igneous, metamorphic, or hydrothermal origins, with V^{3+} occupying

111   octahedral sites of minerals, the majority of which are silicates. V^{5+} minerals are

112   generally of oxidative hydrothermal and weathering origin, and the majority of them are

113   vanadates. In V^{4+} minerals, V is mostly present as VO^{2+}, which can co-occur with V^{3+},

114   vanadate ion (VO_4^{3-}), and many other cations (e.g., Ca^{2+}, Sr^{2+}, Cu^{2+}) and anions (e.g.,

115   SO_4^{2-}, PO_4^{3-}). Thus they are of mixed origins, including metamorphic, hydrothermal, and

116   oxidative weathering phases, such as a variety of minerals including silicates, sulfates,

117   phosphates, and vanadates.

118

119   **NETWORK ANALYSIS OF TERRESTRIAL V MINERALS**

120   Network analysis has been recently applied to study the diversity and distribution of

121   terrestrial minerals (Morrison et al., 2017). Quantification of network metrics, together

122   with clustering analysis, can not only visualize mineral coexistence, but also reveal

123   hidden topologies and phase relations in a mineral network.

124   We perform network analysis on all 219 IMA-approved vanadium minerals, following

125   the methods applied in Morrison et al. (2017), briefly described as follows. The V

126   mineral network is constructed based on mineral co-occurrences. In the network (Fig.

127   1A), each circular node indicates a V mineral, and each link connecting two nodes

128   indicates a coexisting mineral pair. The color of each mineral node indicates the

129   paragenetic mode, the size of each mineral node is proportional to the number of

130   localities, at which that mineral is known, and the length of each link is inversely

131   proportional to the co-occurrence frequency of the mineral pair. Based on these

132   parameters, a force-directed graph of the V mineral network is generated by algorithms

133   running through a number of iterations, displacing the nodes according to the attractive

134   and repulsive forces that they exert on each other, until a layout is found that minimizes

135   the "energy" of the system. Force-directed graphs are browser-based, created using the

136   D3 4.0 d3-force module that simulates physical forces using velocity Verlet integration

137   (Verlet, 1967) and implements the Barnes–Hut approximation (Barnes and Hut, 1986) for

138   performing n-body simulations, analogous to those of planetary systems.

139   To quantify and characterize V mineral networks, we tabulate the V mineral network

140   metrics together with those of Cr and Cu minerals (Table 4). Definition of the network

141   metrics is based on Newman (2013). Given a network with $|N|$ nodes and $|E|$ edges,

142   definitions of the network metrics are described as follows. Edge density is defined as the

143 ratio of |E| divided by potential edge number ($|N|*(|N|-1)/2$). Let C_i represent the number

144 of edges connecting node i, and $C*$ represent max$\{C_1, C_2,\ldots,C_{|N|})\}$, then degree

145 centralization is defined as $\Sigma(C*- C_i)/(|N|^2-3|N|+2)$. Transitivity is defined as 3 times of

146 the ratios between the number of triangles and the number of the connected triples of

147 nodes in the network. Diameter is defined as is the shortest distance between the two

148 most distant nodes in the network. In other words, once the shortest path length from

149 every node to all other nodes is calculated, the diameter is the longest of all the calculated

150 path lengths. Mean distance is defined as the mean of all the calculated path lengths.

151 Calculation of these metrics are based on (Csardi and Nepusz, 2006), and their

152 implications are described as follows. The V mineral network has a low edge density

153 (0.093), meaning that most V mineral species only coexist with a small fraction of V

154 minerals, possibly those of the same paragenetic origin, similar to the other two networks

155 (Morrison et al., 2017). Transitivity is ~0.5, indicating that half of all coexisting mineral

156 pairs also co-occur with a third mineral. The V mineral network is slightly more

157 centralized (degree centralization of ~0.41), and more packed (diameter of 5, and mean

158 distance of ~2.3) than the Cr mineral network, but much less centralized, and less packed

159 than the Cu mineral network. These metrics are consistent with diversified V

160 mineralization in a wide range of paragenetic environments.

161   Cluster analysis employs mineral network data to identify subsets of closely related

162 species—an approach that can reveal previously unrecognized relationships among

163 species. We performed cluster analysis to the 85 commonest V minerals (Figure 1B).

164 Without any supervision, these V mineral nodes separate naturally into seven clusters,

165 faithfully tracking their host ore/rock types. We employed the walktrap algorithm of Pons

166   and Latapy (2006) to detect clusters. This method uses 5-step random network walks,

167   which are more likely to stay within a single cluster because fewer of their edges lead to

168   different clusters.

169   Clustering analysis of V minerals reveals seven different subgroups. The most

170   common V minerals (e.g., carnotite, vanadinite, tyuyamunite) belong to clusters I and II,

171   which are located in the center and connect to most other clusters (Fig. 1B). Cluster I is

172   the largest, composed of 52 minerals associated with U-V deposits, formed through

173   oxidative weathering or low-T hydrothermal alterations, while cluster II is composed of 7

174   V minerals discovered in oxidative zones of Pb-Zn ores. Minerals in each of the other

175   five clusters are found in specific environments or associated with specific ore deposits,

176   and no connection exists among them. Cluster III minerals are mostly Mn vanadates

177   formed in metamorphic Fe-Mn ores (Brugger et al., 2003), and they could co-occur with

178   vanadates from clusters I and II in Mn-deficient zones. Cluster IV is composed of V^{3+}

179   minerals formed during high-grade (>500°C) metamorphism, and its connection to

180   cluster I indicates retrograde alteration or prograde metamorphism (Ito, 1965). Cluster V

181   minerals are associated with bismuth ores formed in pegmatites (Foord, 1996), or via

182   epithermal ores enriched in heavy metals (e.g., Bi, Pb, Te, and occasionally Au; Collier

183   and Plimer, 2002), and thus it is connected to cluster II (Pb-Zn ores). Cluster VI minerals

184   are associated with hydrothermal Cu ores that are rich in sulfides and sulfosalts (e.g.,

185   Nelson, 1939), and minerals in this cluster can be oxidized into those in clusters I and II

186   during ore oxidation (Kampunzu et al., 2009). Cluster VII is isolated from all others,

187   since both minerals (VO^{2+} sulfates) in it are discovered in fossilized woods (Hawthorne

188   et al., 2001; Schindler et al., 2003), distinct from paragenetic environments for minerals

189   in other clusters.

190   In addition to V mineral network and clustering analysis, we constructed a V mineral-

191   locality bipartite network (Fig. 1c) to reveal mineral diversity at each locality. In this

192   network, each circular node indicates a V mineral (non-black) or a locality (black), and

193   each link connecting two nodes indicates occurrence of one mineral at one locality.

194   Similar to the V mineral network, the V bipartite network is also force-directed,

195   generated by algorithms running through a number of iterations, displacing the nodes

196   according to the attractive and repulsive forces that they exert on each other. There are

197   only a few V minerals that are most common located at the center of the diagram, each

198   connecting to many locality nodes. By contrast, most V minerals are situated along the

199   peripheral areas, and are connected to only one or two localities. The bipartite network

200   thus embodies a Large Number of Rare Events (LNRE) frequency distribution (Baayen

201   2001; Evert and Baroni 2008) for terrestrial V minerals, i.e., a few V mineral species

202   occur at many localities, but most V minerals are present only at a few localities.

203   Furthermore, the bipartite network also reveals many rare minerals that are formed in

204   paragenetic environments unidentified by clustering analysis. For instance, a couple

205   locality nodes of volcanic fumaroles, Izalco Volcano in El Salvador and Tolbachik

206   Volcano in Kamchatka of Russia, are observed outlying from most others (Fig. 1c), and

207   each is connected to a group of isolated mineral nodes. This topology indicates that V

208   minerals seldom occur in volcanic fumaroles but, when they do, they are present as a

209   variety of rare species.

210

211 **STATISTICAL ANALYSIS OF TERRESTRIAL V MINERALS**

212   Hystad et al. (2015) discovered that the distribution of all terrestrial minerals conforms

213 to a LNRE frequency distribution. This distribution pattern was later reported for the

214 minerals of carbon, boron, cobalt, chromium, and other elements (Hazen et al. 2016a,

215 2016b; Grew et al. 2016; 2016b; Liu et al., 2017). We modeled the frequency distribution

216 of vanadium minerals based on the numbers of known localities for each of the 219

217 approved vanadium minerals. The easiest approach to estimate the number of localities

218 for each species is to interrogate the crowd-sourced data resource mindat.org, which

219 tabulates locality information for every mineral species. To minimize errors arising from

220 uncritical use of mindat.org locality data, we examined and updated the raw V-mineral

221 species-locality data by removing geographically redundant mindat.org localities, while

222 adding missing localities cited in the *Handbook of Mineralogy* (Anthony et al., 2003) but

223 not in mindat.org (Hazen et al., 2016b; Liu et al., 2017).

224   There are 5437 V-mineral species-locality data pairs in total, with 66 species recorded

225 at only one locality, an additional 33 species at exactly 2 localities, and 22 species at

226 exactly 3 localities (Table 1). By contrast, the 11 most common vanadium minerals

227 account for more than 70% of all species-locality data. This pattern of species distribution

228 among localities, with a few common species and many more rare ones, is typical for the

229 whole set, as well as for various subsets of minerals (Hazen et al. 2015a, 2016a; Hystad

230 et al. 2015b; Grew et al. 2016).

231   The V-mineral species-locality data are fit to a finite Zipf-Mandelbrot (fZM) model

232 (Hystad et al. 2015a). The fZM parameters for bulk V-mineral species ($\alpha = 0.4855164$; A

233 $= 0.000063038$; B $= 0.1490914$; P-value $= 0.17$) facilitate modeling of a V-mineral

234   accumulation curve (Fig. 2), with a prediction of at least 307 vanadium minerals in total.

235   In other words, at least 88 V minerals on Earth have not been described. Errors of the

236   fZM model are estimated in a brute-force Monte-Carlo method for bulk V-mineral

237   species, described as follows. Occurrence probabilities were first calculated for each

238   species in the population of 293 V minerals (including both existing and missing species).

239   Based on these probabilities, 500 random samples of size N=5437 (species-locality pairs)

240   were taken from this population. For each sample fZM LNRE model was refitted and the

241   expected population size S for each sample was calculated. The standard deviation of

242   these population size S of all 500 random samples was calculated as an error estimation

243   of the fZM model. The resulting analysis suggests a standard deviation of 30 species for

244   bulk V minerals.

245   **IMPLICATIONS: THE "MISSING" MINERALS OF VANADIUM**

246   The 219 known V-mineral species represent only a small fraction of the thousands of

247   known inorganic V compounds [International Crystal Structure Database (http://icsd.fiz-

248   karlsruhe.de)]. Vanadium, as all other elements, has the potential to form thousands of

249   mineral species (Hazen et al., 2015b); however, far fewer V mineral species have formed

250   on Earth because of the special geochemical conditions required to concentrate

251   vanadium. Prediction of the exact chemistry, location, and paragenesis of most new V

252   mineral species is unlikely. However, characteristics of the possible missing V minerals,

253   including their chemistry and paragenesis, can be constrained by LNRE modeling of V

254   mineral subsets.

255   We first applied LNRE-fZM models and performed error analysis to subsets of

256   vanadium minerals categorized by the V oxidation state (Table 5). For V^{5+} minerals, the

257   model predicts that at least 38 ± 21 (1 sigma) species await discovery. However, for V^{3+}

258   and V^{4+} minerals, the fZM model predicts unreasonable numbers of undiscovered species,

259   and the Monte-Carlo error analysis cannot render convergent results (Table 5). This

260   problem is likely due to the fact that the sample size is small (554 and 495 species-

261   locality pairs for V^{3+} and V^{4+} minerals, respectively) but relatively large (4678 species-

262   locality pairs) for V^{5+} minerals.

263   In addition, we applied LNRE-fZM models and performed error analysis to V mineral

264   subsets of rock-forming species (i.e., minerals composed of Si, Al or Ti) and non rock-

265   forming V-O salts (i.e., minerals containing V, O and devoid of Si, Al and Ti). Note these

266   two subsets are independent from those categorized based on vanadium valences. For

267   rock-forming species, the model predicts that at least 26 ± 12 (1 sigma) species are

268   missing. In comparison, for non rock-forming V-O salts, the model suggest at least $52 \pm$

269   19 (1 sigma) are yet to be discovered.

270   Furthermore, we applied LNRE-fZM models and performed error analysis on various

271   subsets of V mineral defined by cluster analysis. To be specific, we analyzed one subset

272   that includes V minerals discovered in U-V ore deposits, and a second subset that

273   includes all other species. All non-U-V-deposit clusters are combined for LNRE

274   modeling since the sample size is too small in each. For V minerals from U-V deposits,

275   the model predicts only 9 ± 8 (1 sigma) undiscovered species, suggesting most V

276   minerals in U-V deposits have been documented. This prediction is not surprising since V

277   mineral species (e.g., carnotite, tyuyamunite) in U-V deposits are typically colorful and

278   well-crystallized, and thus easier to be collected and identified in hand specimen. In

279   contrast, many more V minerals, up to 76 ± 34 (1 sigma) species, are yet to be discovered

280   for non-U-V deposits. The modeling result is consistent with the bipartite network (Fig.

281   1c) which shows that many rare V minerals are formed in uncommon paragenetic

282   environments (e.g., volcanic fumaroles).

283   To summarize, for the missing V minerals, the LNRE modeling on different V-

284   mineral subsets suggest that about a half may be V^{5+} species, and the other half are $V^{3+/4+}$

285   minerals; a third may be present as rock-forming minerals, and two thirds may exist as

286   non rock-forming V-O salts; and most species are likely to be discovered in paragenetic

287   environments other than U-V ore deposits.

288   In addition to LNRE predictions, we also tabulate 660 synthetic V compounds

289   (Supplementary Table S1) that have not been discovered in nature, but are speculated to

290   occur on Earth (or on other highly differentiated planets) as new mineral species. These

291   potential V minerals include 7 oxides, 26 sulfides, 6 silicates, 16 uranates, 59

292   sulfur/selenium/tellurium-oxy acid salts (e.g., sulfates, sulfites, selenates, tellurates), 102

293   phosphates, 16 arsenates, 70 halides, and 358 others. Most of the stable V silicates have

294   been discovered in nature (37 minerals), and only a few (6 species) are known

295   exclusively as synthetic species. V valences of synthetic V oxides stable at Earth's

296   surface are between +3 and +5, similar to those of discovered V oxides minerals (e.g.,

297   karelianite, paramontroseite, and shcherbinaite). We speculate that V oxides and silicates

298   known only as synthetic compounds are most likely to be discovered in metamorphic

299   rocks, fumaroles, or hydrothermal U-V deposits, similar to previously discovered species.

300   Synthetic stable V-bearing sulfides could contain V^{3+}, V^{4+}, or V^{5+}, many of which share

301   similar crystal structures to V/transition metal minerals (Table S1). For instance, two V

302   sulfides share structures similar to colimaite, and a group of synthetic V sulfides exhibit a

303   spinel structure, similar to some metal Cr sulfide minerals (e.g., brezinaite, kalininite; Liu

304   et al., 2017). These synthetic V sulfides, if present in nature, are likely to be of

305   hydrothermal origin, since most of V sulfide minerals are found primarily in

306   hydrothermal deposits (Table 1). Synthetic V uranates (U^{6+}) yet to be discovered in

307   nature are all anhydrous (Table S1), whereas all discovered V uranate minerals are

308   hydrous species, of hydrothermal or secondary weathering origin. Most of the synthetic

309   experiments are performed in anhydrous environments, whereas water is ubiquitously

310   present at the Earth's surface. Therefore, the chances of finding these anhydrous synthetic

311   species in nature are very small.

312   Association of V with some common anions (e.g., sulfates, phosphates, arsenates,

313   selenates, tellurates, halides) is observed not only in many minerals (Table 1), but also in

314   a variety of synthetic compounds (Table S1). Abundances of both minerals and synthetic

315   crystals in this group imply a number of new V minerals remain to be discovered in

316   hydrothermal, sedimentary, or secondary weathering deposits. In comparison, V

317   carbonates and nitrates are very rare in both discovered minerals and synthetic

318   compounds, indicating very small chances of finding these species in nature.

319   The remaining synthetic V compounds are dominantly vanadates (Table S1). Note that

320   for both mineral and synthetic compounds, the number of phosphates, although quite

321   high, is significantly less than that of vanadates. This difference is due to the fact that

322   crystal chemical behaviors of V^{5+} and P^{5+} are similar but not identical (Schindler et al.,

323   2000). A few of the vanadate synthetic crystals share similar structures to known V

324   minerals (e.g., cavoite, blossite, and ansermetite). However, the majority of them possess

325   different crystal structures. Chemical compositions of the synthetic vanadates are very

326   diverse, containing most lithophile and chalcophile elements, as well as some siderophile

327   elements, as essential elements. Based on their chemistry (Table S1) and the paragenesis

328   of current vanadate minerals (Table 1, Figure 1B), we propose that these synthetic

329   vanadates may be discovered in oxidized zones of Pb-Zn or other heavy metal (e.g., Bi,

330   Te) ore deposits.

331

332

333   **ACKNOWLEDGEMENTS**

340

341

342

343

344

345

346

347

348

349
350   **Figure 1.** (*A*) Force-directed network graphs of 219 vanadium minerals sorted by
351   paragenetic mode (data and mode definition are from Table 1). The dominant species
352   are the minerals formed through secondary oxidative weathering (group 7). Most
353   minerals tend to cluster with those of the same paragenetic mode. (*B*) Cluster analysis
354   of the most common 85 vanadium minerals reveals segregation into 7 groups, see text
355   for discussion. In the cluster analysis, we apply the walktrap algorithm (Pons and
356   Latapy, 2006) of 'igraph' package in R to detect clusters. With this algorithm, we
357   perform random walks on the V mineral graph for 5 steps, and the minerals separate
358   naturally into eight clusters (cluster IV include two close subclusters, we combine
359   them together because minerals in them share very similar chemical signatures and
360   paragenesis). Note in this graph we include only V minerals that occur at least 3
361   localities and co-occur at least 3 localities with other V minerals. (*C*) Force-directed
362   bipartite network graphs of 219 vanadium minerals and their localities (data are from
363   Tables 1 and 2). The localities are indicated by black nodes, while mineral nodes are
364   colored based on paragenetic mode (mode definition are from Table 1). The bipartite
365   network visualizes LNRE distribution of V minerals (see text for discussion).
366

368
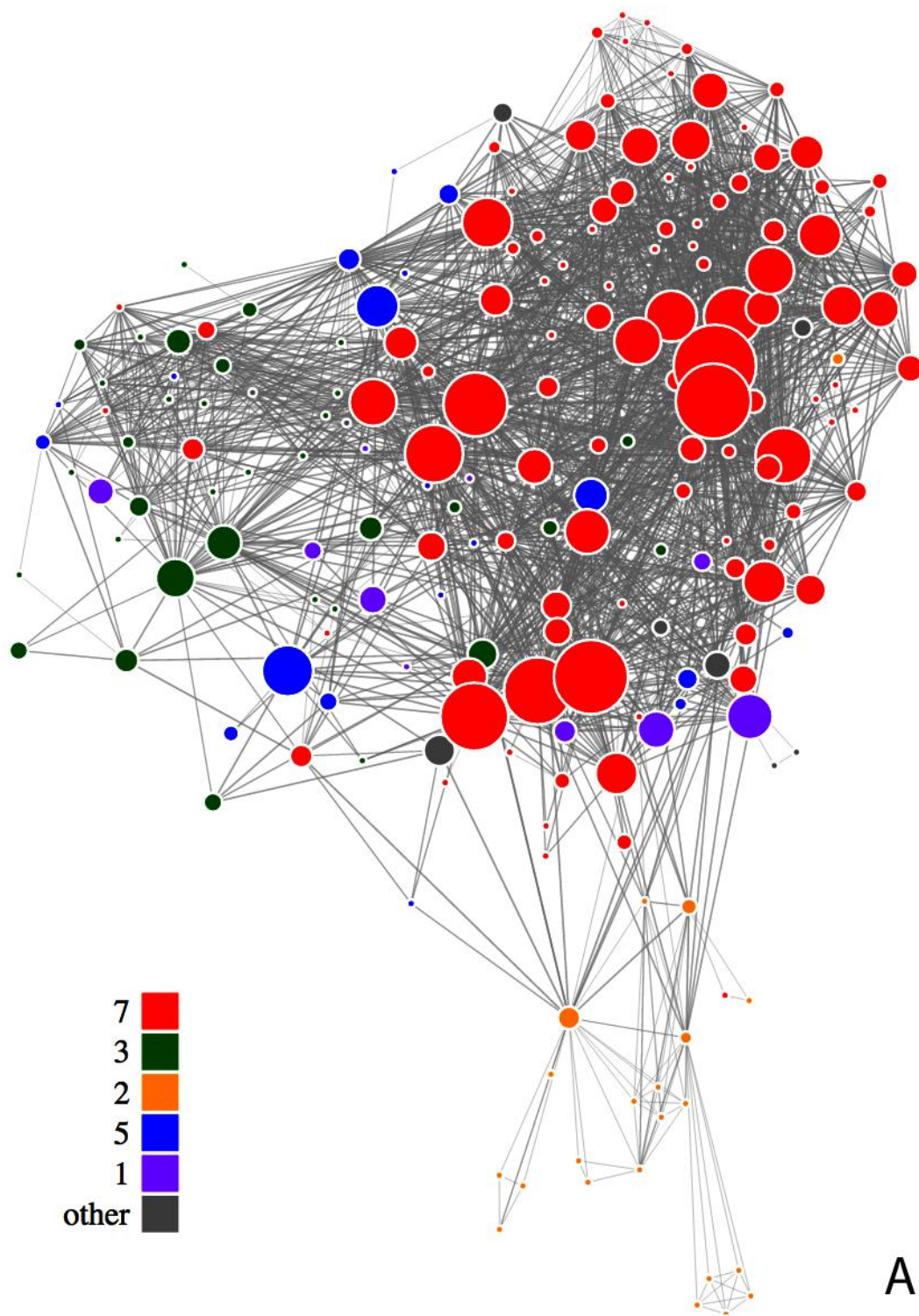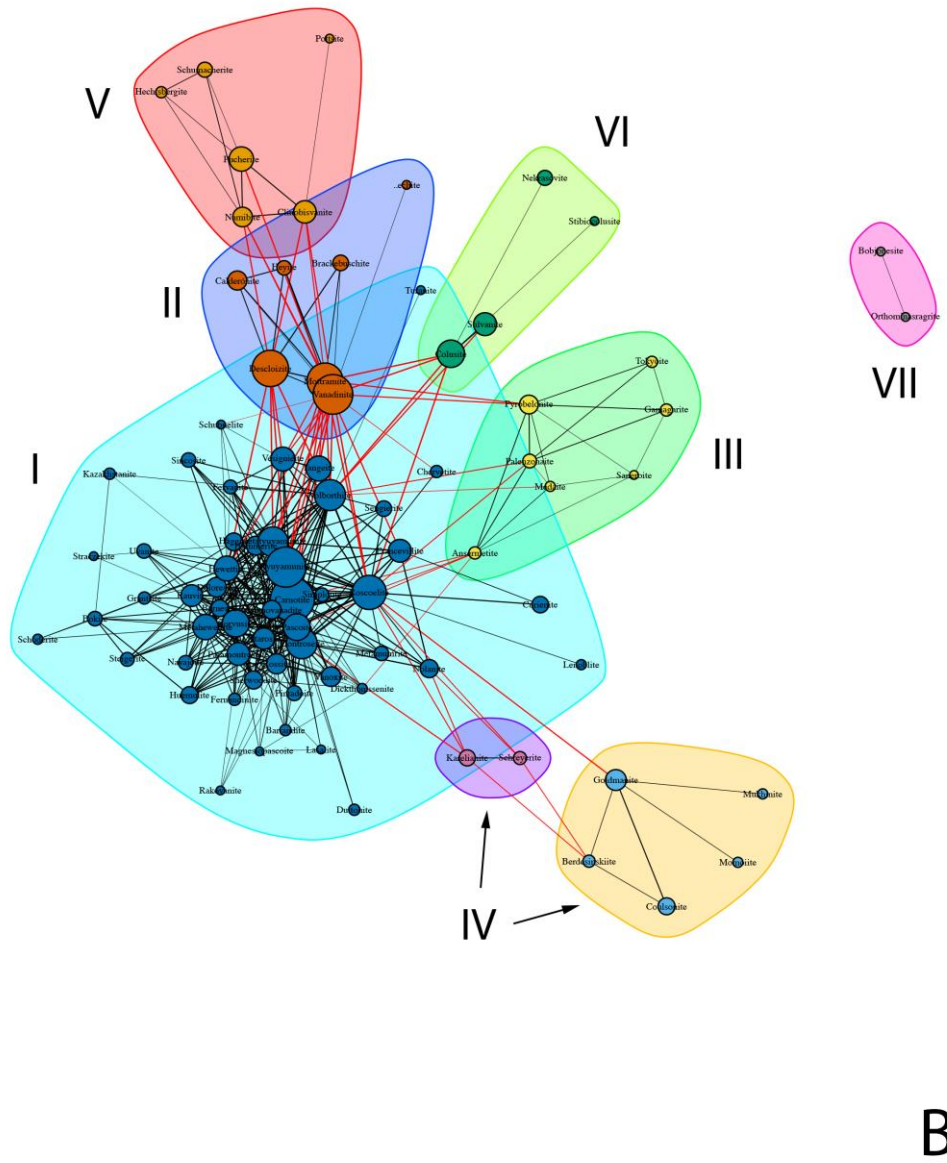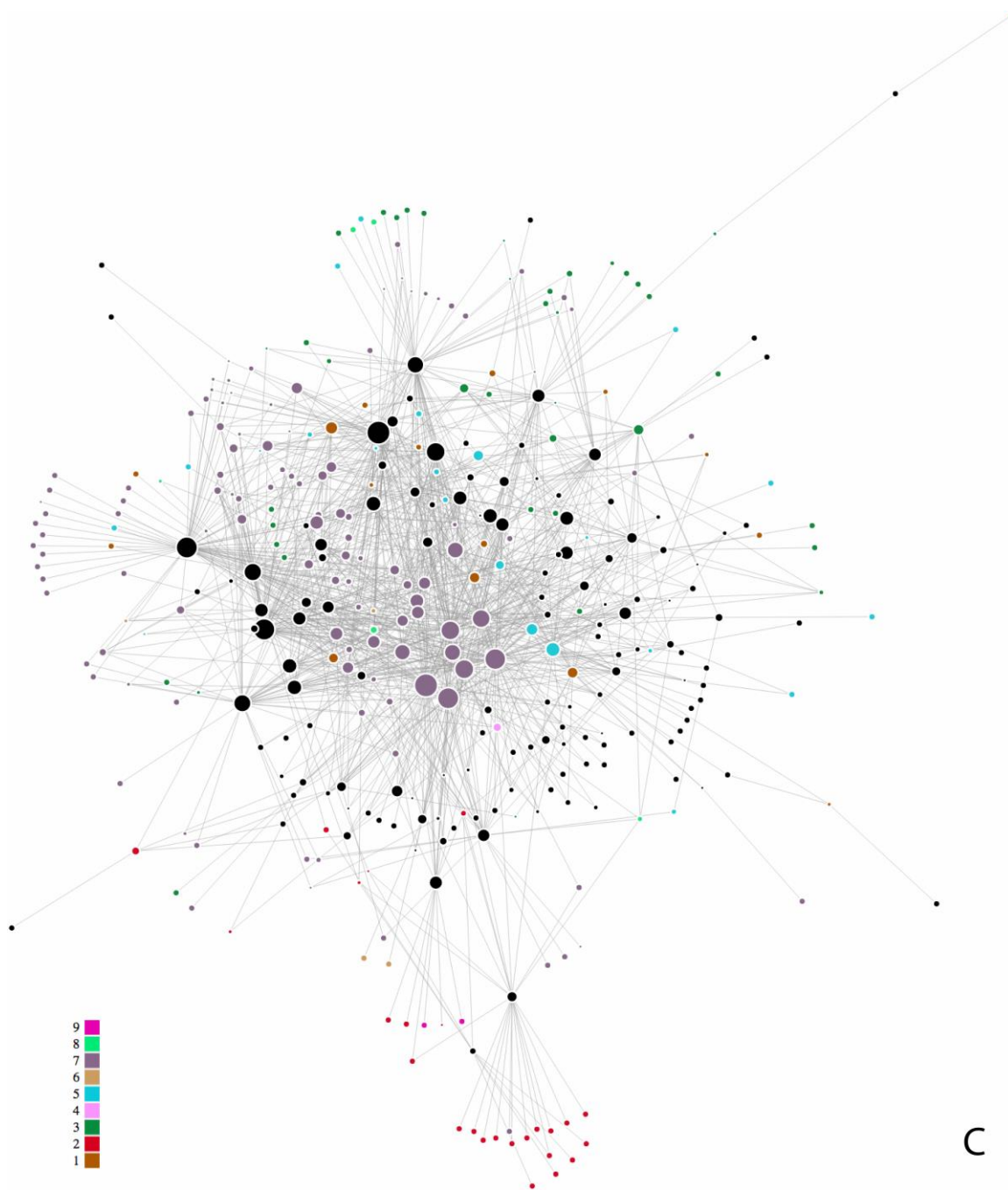
369

370

371

372

373

374

375

376

377 **Figure 2.** (*A*) Frequency spectrum analysis of 219 V-bearing minerals, with 5437

378 individual mineral-locality data (from mindat.org as of 15 April 2016), a finite Zipf-

379 Mandelbrot (fZM) method to model the number of mineral species for minerals found at

380 exactly 1 to 15 localities (Hystad et al. 2015a). (*B*) This model facilitates the prediction of

381 the mineral species accumulation curve (upper curve, "all"), which plots the number of

382 expected V mineral species (*y*-axis) as additional mineral species/locality data (*x*-axis)

383 are discovered. The vertical dashed line indicates data recorded as of 15 April 2016 in

384 mindat.org, as well as locality data from the *Handbook of Mineralogy* (Anthony et al.

385 2003) and systematic searching under each mineral name in Georef. The model also

386 predicts the varying numbers of mineral species known from exactly one locality (curve

387 1) or from exactly two localities (curve 2). Note that the number of mineral species from

388 only one locality is now decreasing, whereas the number from two localities is now

389 increasing. We predict that the number of minerals known from two localities will

390 surpass those from one locality when the number of species-locality data exceeds

391 ~13000.

392
393
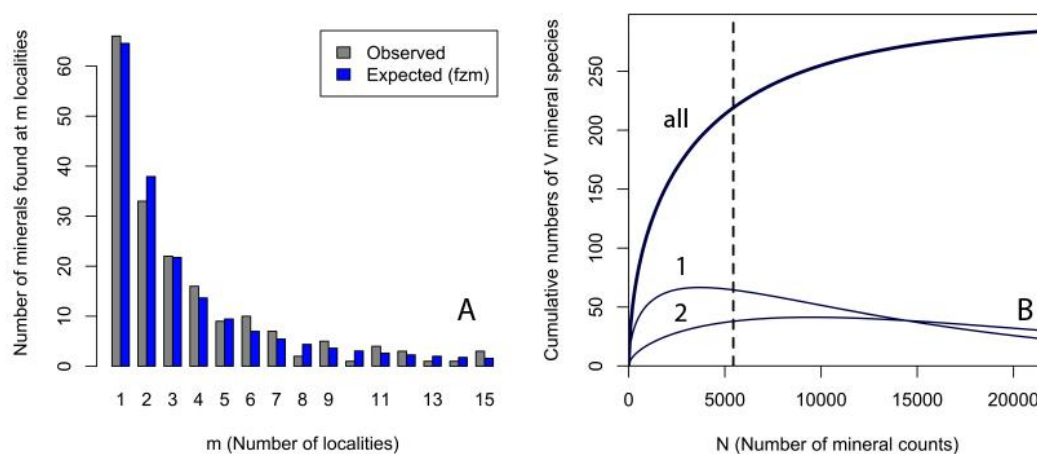
394
395
396
397
398
399
400

REFERENCES CITED

401
402
403

404 Anthony, J.W., Bideaux, R.A., Bladh, K.W., and Nichols, M.C. (2003) Handbook of

405   Mineralogy. Volume V. Borates, Carbonates, Sulfates. Tucson, Arizona: Mineral Data

406   Publishing.

407 Baayen, R.H. (2001) Word Frequency Distributions. Dordrecht, The Netherlands:

408   Kluwer.

409 Barnes, J. and Hut, P. (1986) A hierarchical O(N log N) force-calculation algorithm.

410   Nature, 324, 446-449.

411 Brugger, J., Berlepsch, P., Meisser, N., and Armbruster, T. (2003) Ansermetite,

412      $MnV_2O_6 \cdot 4H_2O$, a new mineral species with V^{5+} in five-fold coordination from Val

413   Ferrera, Eastern Swiss Alps. The Canadian Mineralogist, 41, 1423-1431.

414 Collier, J.B. and Plimer, I.R. (2002) Supergene clinobisvanite pseudomorphs after

415   supergene dreyerite from Lively's Mine, Arkaroola, South Australia. Neues Jahrbuch

416   für Mineralogie-Monatshefte, 2002, 401-410.

417 Csardi, G., Nepusz, T. (2006) The igraph software package for complex network

418   research. InterJournal, Complex Systems, 1695, 1-9.

419 Curtis, C.D. (1964) Applications of the crystal-field theory to the inclusion of trace

420   transition elements in minerals during magmatic differentiation. Geochimica et

421   Cosmochimica Acta, 28, 389-403.

422 Downs, R.T. (2006) The RRUFF Project: an integrated study of the chemistry,

423   crystallography, Raman and infrared spectroscopy of minerals. Program and Abstracts

424   of the 19th General Meeting of the International Mineralogical Association in Kobe,

425   Japan. O03-13.

426   Evert, S. and Baroni, M. (2008) Statistical Models for Word Frequency Distributions,

427   Package zipfR.

428   Foord, E.E. (1996) Clinobisvanite, eulytite, and namibite from the Pala pegmatite district,

429   San Diego Co., California, USA. Mineralogical Magazine, 60, 387-388.

430   Grew, E.S., Krivovichev, S.V., Hazen, R.M., and Hystad, G. (2016) Evolution of

431   structural complexity in boron minerals. Canadian Mineralogist, in press.

432   Gummow, B. (2011) Vanadium: environmental pollution and health effects.

433   Encyclopedia of Environmental Health, pp.628-636.

434   Hawthorne, F.C., Schindler, M., Grice, J.D., and Haynes, P. (2001) Orthominasragrite,

435         $V^{4+}O(SO_4)(H_2O)_5$, a new mineral species from Temple Mountain, Emery County,

436   Utah, USA. The Canadian Mineralogist, 39, 1325-1331.

437   Hazen, R.M., Grew, E.S., Downs, R.T., Golden, J., and Hystad, G. (2015a) Mineral

438   ecology: Chance and necessity in the mineral diversity of planets. Canadian

439   Mineralogist, 53, 295-324

440   Hazen, R.M., Hystad, G., Downs, R.T., Golden, J., Pires, A., and Grew, E.S. (2015b)

441   Earth's "missing" minerals. American Mineralogist, 100, 2344-2347.

442   Hazen, R.M., Hummer, D.R., Hystad, G., Downs, R.T., and Golden, J.J. (2016a) Carbon

443   mineral ecology: Predicting the undiscovered minerals of carbon. American

444   Mineralogist, 101, 889-906.

445   Hazen, R.M., Hystad, G., Golden, J.J., Hummer, D.R., Liu C., Downs, R.T., Morrison

446   S.M., and Grew, E.S. (2016b) Cobalt mineral ecology. American Mineralogist, in

447   press.

448   Huang, J.-H., Huang, F., Evans, L., Glasauer, S. (2015) Vanadium: Global

449   (bio)geochemistry. Chemical Geology, 417: 68-89.

450   Hystad, G., Downs, R.T., and Hazen, R.M. (2015a) Mineral frequency distribution data

451   conform to a LNRE model: Prediction of Earth's "missing" minerals. Mathematical

452   Geosciences, 47, 647-661.

453   Hystad, G., Downs, R.T., Grew, E.S., and Hazen, R.M. (2015b) Statistical analysis of

454   mineral diversity and distribution: Earth's mineralogy is unique. Earth and Planetary

455   Science Letters, 426, 154-157.

456   Hystad, G., Downs, R.T., Hazen, R.M., and Golden, J.J. (2016) Relative abundances of

457   mineral species: A statistical measure to characterize Earth-like planets based on

458   Earth's mineralogy. Mathematical Geosciences. DOI: 10.1007/s11004-016-9661-y

459   Ito, J. (1965) Synthesis of vanadium silicates: Haradaite, Goldmanite and Roscoelite.

460   Mineralogical Journal, 4, 299-316.

461   Lee, C.T.A., Brandon, A.D., and Norman, M. (2003) Vanadium in peridotites as a proxy

462   for paleo-fO2 during partial melting: prospects, limitations, and implications.

463   Geochimica et Cosmochimica Acta, 67, 3045-3064.

464   Liu C., Hystad, G., Golden, J.J., Hummer, D.R., Downs, R.T., Morrison S.M., Ralph J.,

465   and Hazen, R.M. (2017) Chromium mineral ecology. American Mineralogist, 102,

466   612-619.

467   Kampunzu, A.B., Cailteux, J.L.H., Kamona, A.F., Intiomale, M.M., and Melcher, F.

468   (2009) Sediment-hosted Zn–Pb–Cu deposits in the Central African Copperbelt. Ore

469   Geology Reviews, 35, 263-297.

470   Koljonen, T. (Ed.). 1992. The Geochemical Atlas of Finland, part 2 - Till. Geological

471   Survey of Finland, 218 pp.

472   Mielke, J.E. (1979) Composition of the Earth's crust and distribution of the elements.

473   Review of research on modern problems in Geochemistry. UNESCO Report, Paris,

474   pp.13-37.

475   Morrison S.M., Liu C., Eleish A., Prabhu A., Li C., Ralph J., Downs, R.T., Golden, J.J.,

476   Fox P., and Hazen, R.M. (2017) Network Analysis of Mineralogical Systems.

477   American Mineralogist, 102, 1588-1596

478   Mukherjee, B., Patra, B., Mahapatra, S., Banerjee, P., Tiwari, A. and Chatterjee, M.

479   (2004) Vanadium—an element of atypical biological significance. Toxicology letters,

480   150, 135-143.

481   National Research Council (2008) Minerals, Vitical Minerals, and the U.S. Economy.

482   Washington, DC: Natrional Research Council of the National Academies.

483   Nelson, R. (1939) Colusite-its occurrence, paragenesis and genetic significance.

484   American Mineralogist, 24, 369-376.

485   Newman, M.E.J. (2013) Networks: An Introduction. Oxford University Press, New York.

486   Orcutt, M. (2011) Material world. Technology Review, [July/August 2011], 24-25.

487   Pons, P. and M. Latapy (2005) Computing communities in large networks using random

488   walks. International Symposium on Computer and Information Sciences, Springer. pp.

489   284-293

490   Rehder, D. (2008) Is vanadium a more versatile target in the activity of primordial life

491   forms than hitherto anticipated? Org. Biomol. Chem. 6, 957–964.

492   Righter, K., Sutton, S.R., Danielson, L., Pando, K., and Newville, M. (2016) Redox

493   variations in the inner solar system with new constraints from vanadium XANES in

494   spinels. American Mineralogist, 101, 1928-1942.

495   Rudnick, R. L. and D. M. Fountain (1995) Nature and composition of the continental

496   crust: a lower crustal perspective. Reviews of geophysics 33, 267-309.

497   Rudnick, R.L. and Gao, S. (2005) Composition of the continental crust. In Rudnick, R.L.

498   (ed.) The Vust, volume 3 of Holland, H.D. & Turekian, K.K. (eds.) Treatise on

499   Geochemistry, p. 1-64. Oxford, UK: Elsevier-Pergamon.

500   Schindler, M., Hawthorne Frank, C. (1999) Schubnelite, [$Fe^{3+}(V^{5+}O_4)(H_2O)$], a novel

501   heteropolyhedral framework mineral, American Mineralogist, pp. 665.

502   Schindler, M., Hawthorne, F.C., Baur, W.H. (2000) Crystal Chemical Aspects of

503   Vanadium: Polyhedral Geometries, Characteristic Bond Valences, and Polymerization

504   of (VO_n) Polyhedra. Chemistry of Materials, 12, 1248-1259.

505   Schindler, M., Hawthorne, F.C., Huminicki, D.M., Haynes, P., Grice, J.D., and Evans,

506   H.T. (2003) Bobjonesite, $V^{4+}O(SO_4)(H_2O)_3$, a new mineral species from Temple

507   Mountain, Emery County, Utah, USA. The Canadian Mineralogist, 41, 83-90.

508   Verlet, L. (1967) Computer "experiments" on classical fluids. I. Thermodynamical

509   properties of Lennard−Jones molecules. Physical Review, 159, 98-103.

510

511

Table 1: IMA recognized terrestrial minerals of vanadium, with numbers of recorded occurrences in parentheses, chemical formulas, paragenetic modes, V valences, and selected mineral localities (see Table 2 for key to localities). This table includes only minerals with V occupying more than 50% of a symmetrically distinct crystallographic site. Mineral and locality data were compiled from MinDat.org as of April 15, 2016.

# Name (# Localities)	Formula	Paragenetic mode*	V valences	Biotic	Localities
1 Vanadium(2)	V	2	0		53
2 Sulvanite(41)	Cu_3VS_4	5	2		8, 34, 56, 60
3 Batisivite(2)	$BaTi_6(V,Cr)_8Si_2O_{29}$	3	3		67
4 Beckettite(1)	$Ca_2V_6Al_6O_{20}$	9	3		75
5 Berdesinskiite(5)	V_2TiO_5	7	3	X	30, 44, 52
6 Burnettite(1)	$CaVAlSiO_6$	9	3		75
7 Byrudite(1)	$Be(V,Ti)_3O_6$	1	3		81
8 Cassagnaite(1)	$Ca_4Fe_4V_2(OH)_6O_2(Si_3O_{10})(SiO_4)_2$	3	3		45
9 Chernykhite(3)	$BaV_2(Si_2Al_2)O_{10}(OH)_2$	5	3		8, 17, 56
10 Cortesognoite(1)	$CaV_2Si_2O_7(OH)_2·H_2O$	3	3		3
11 Coulsonite(15)	FeV_2O_4	4	3		44
12 Goldmanite(29)	$Ca_3V_2(SiO_4)_3$	3,6	3		1, 30, 62
13 Greenwoodite(1)	$Ba_{2-x}(VOH)_xV_9(Fe^{3+},Fe^{2+})_2Si_2O_{22}$	3	3		67
14 Hanjiangite(1)	$Ba_2Ca(VAl)(AlSi_3O_{10})(OH)_2F(CO_3)_2$	5	3		56
15 Karelianite(13)	V_2O_3	3,8	3	X	5, 30, 44, 47, 49
16 Kyzylkumite(2)	$Ti_2VO_5(OH)$	5	3		44
17 Magnesiocoulsonite(1)	MgV_2O_4	3	3		30
18 Mannardite(9)	$Ba(Ti_6V_2)O_{16}$	1,5	3		77
19 Momoiite(4)	$Mn_3V_2(SiO_4)_3$	3	3		62
20 Mukhinite(6)	$Ca_2Al_2V(Si_2O_7)(SiO_4)O(OH)$	3	3		49

21	Nagashimalite(2)	$Ba_4(V,Ti)_4(O,OH)_2[B_2Si_8O_{27}]Cl$	3	3		64
22	Natalyite(3)	$NaVSi_2O_6$	3	3		26, 30
23	Nolanite(19)	$(V,Fe,Fe,Ti)_{10}O_{14}(OH)_2$	5	3		4, 5, 26, 36, 69
24	Oxy-vanadium-dravite(1)	$NaV_3(V_4Mg_2)Si_6O_{18}(BO_3)_3(OH)_3O$	3	3		74
25	Poppiite(3)	$Ca_2(V,Fe,Mg)V_2(Si,Al)_3(O,OH)_{14}$	3	3		1
26	Roscoelite(242)	$KV_2(Si_3Al)O_{10}(OH)_2$	7	3	X	1, 2, 3, 4, 5
27	Schreyerite(9)	$V_2Ti_3O_9$	3,4	3		26, 30, 52
28	Springcreekite(1)	$BaV_3(PO_4)(PO_3OH)(OH)_6$	5	3		57
29	Tivanite(2)	$TiVO_3(OH)$	5	3		69
30	Tomichite(2)	$V_4Ti_3AsO_{13}(OH)$	5	3		69
31	Vanadio-oxy-chromium-dravite(1)	$NaV_3(Cr_4Mg_2)(Si_6O_{18})(BO_3)_3(OH)_3O$	3	3		1, 3
32	Vanadio-oxy-dravite(1)	$NaV_3(Al_4Mg_2)(Si_6O_{18})(BO_3)_3(OH)_3O$	3	3		80
33	Vanadiocarpholite(1)	$MnVAlSi_2O_6(OH)_4$	8	3	X	30
34	Vanadoallanite-(La)(1)	$CaLaVAlFe(Si_2O_7)(SiO_4)O(OH)$	3	3		82
35	Vanadoandrosite-(Ce)(1)	$MnCeVAlMnO(Si_2O_7)(SiO_4)(OH)$	3	3		66
36	Vuorelainenite(7)	MnV_2O_4	3	3		52, 62, 66
37	Häggite(19)	$VVO_2(OH)_3$	7	3,4	X	1, 9, 12, 16, 20
38	Montroseite(140)	$(V,Fe,V)O(OH)$	7,8	3,4	X	2, 4, 5, 7, 11
39	Oxyvanite(2)	V_3O_5	3	3,4		3, 74
40	Zoltaiite(1)	$BaV_2V_{12}Si_2O_{27}$	3	3,4		67
41	Anorthominasragrite(2)	$VO(SO_4)\cdot5H_2O$	7	4	X	22
42	Bariosincosite(2)	$Ba(VO)_2(PO_4)_2\cdot4H_2O$	5	4		57
43	Bassoite(1)	$SrV_3O_7\cdot4H_2O$	3	4		3
44	Bavsiite(1)	$Ba_2V_2O_2[Si_4O_{12}]$	3	4		78
45	Bobjonesite(3)	$VOSO_4\cdot3H_2O$	7	4	X	22
46	Cavansite(15)	$CaVOSi_4O_{10}\cdot4H_2O$	2,5	4		71
47	Cavoite(1)	CaV_3O_7	5	4		1
48	Cloncurryite(1)	$Cu_{0.5}(VO)_{0.5}Al_2(PO_4)_2F_2\cdot5H_2O$	7	4	X	86
49	Doloresite(26)	$V_3O_4(OH)_4$	7	4	X	2, 7, 11, 13, 19

50	Duttonite(7)	$VO(OH)_2$	7	4	X	5, 11
51	Evdokimovite(1)	$Tl_4(VO)_3(SO_4)_5 \cdot 5H_2O$	2	4		79
52	Haradaite(3)	$SrVSi_2O_7$	3	4		1
53	Karpovite(1)	$Tl_2VO(SO_4)_2 \cdot H_2O$	2	4		72
54	Lenoblite(5)	$V_2O_4 \cdot 2H_2O$	7	4	X	3, 5, 6
55	Minasragrite(2)	$VO(SO_4) \cdot 5H_2O$	7,8	4	X	27
56	Orthominasragrite(3)	$VO(SO_4) \cdot 5H_2O$	7,8	4	X	22
57	Paramontroseite(41)	VO_2	7	4	X	2, 4, 11, 13, 16
58	Patrónite(6)	VS_4	8	4	X	27, 60
59	Pauflerite(3)	$VO(SO_4)$	2	4		53
60	Pentagonite(4)	$CaVOSi_4O_{10} \cdot 4H_2O$	2,7	4	X	71
61	Phosphovanadylite-Ba(1)	$BaV_4P_2O_{10}(OH)_6 \cdot 12H_2O$	6,8	4	X	70
62	Phosphovanadylite-Ca(1)	$CaV_4P_2O_{10}(OH)_6 \cdot 12H_2O$	6,8	4	X	70
63	Simplotite(9)	$CaV_4O_9 \cdot 5H_2O$	7,8	4	X	4, 11, 13, 25
64	Sincosite(11)	$Ca(VO)_2(PO_4)_2 \cdot 4H_2O$	8	4	X	9, 12, 25, 70
65	Stanleyite(2)	$VO(SO_4) \cdot 6H_2O$	7	4	X	27
66	Stibivanite(3)	Sb_2VO_5	3,5,6,7	4		47
67	Suzukiite(4)	$BaVSi_2O_7$	3	4		63, 64, 78
68	Vanadomalayaite(1)	$CaVO(SiO_4)$	3	4		1
69	Watatsumiite(1)	$KNa_2LiMn_2V_2Si_8O_{24}$	3	4		63
70	Yushkinite(1)	$(Mg,Al)(OH)_2VS_2$	5	4		60
71	Bannermanite(4)	$(Na,K)_xV_xV_{6-x}O_{15}(0.5< x<0.9)$	2	4,5		28, 61
72	Bariandite(6)	$Al_{0.6}(V,V)_8O_{20} \cdot 9H_2O$	7	4,5	X	5, 7, 14, 18, 27
73	Bluestreakite(1)	$K_4Mg_2(V_2V_8O_{28}) \cdot 14H_2O$	7	4,5	X	32
74	Bokite(6)	$(Al,Fe)_{1.3}(V,V,Fe)_8O_{20} \cdot 7.5H_2O$	7,8	4,5	X	2, 8, 17, 29
75	Corvusite(83)	$(Na,Ca,K)_{1-x}(V,V,Fe)_8O_{20} \cdot 4H_2O$	7	4,5	X	2, 4, 5, 7, 8
76	Fernandinite(6)	$(Ca,Na,K)_{0.9}(V,V,Fe,Ti)_8O_{20} \cdot 4H_2O$	7,8	4,5	X	2, 14, 23, 27
77	Gatewayite(1)	$Ca_6(AsV_3V_9As_6O_{51}) \cdot 31H_2O$	7	4,5	X	35
78	Grantsite(5)	$(Na,Ca)_{2+x}(V,V)_6O_{16} \cdot 4H_2O$	7,8	4,5	X	20

79	Hendersonite(3)	$Ca_{1.3}(V,V)_6O_{16} \cdot 6H_2O$	7	4,5	X	13, 15
80	Kazakhstanite(5)	$Fe_5V_3V_{12}O_{39}(OH)_9 \cdot 8.5H_2O$	7	4,5	X	8, 9, 12, 17
81	Melanovanadite(19)	$Ca(V,V)_4O_{10} \cdot 5H_2O$	7,8	4,5	X	4, 5, 10, 11, 13
82	Morrisonite(1)	$Ca_{11}(AsV_2V_{10}As_6O_{51})_2 \cdot 78H_2O$	7	4,5	X	35
83	Nashite(2)	$Na_3Ca_2([V_9V]O_{28}) \cdot 24H_2O$	7	4,5	X	10, 15
84	Packratite(1)	$Ca_{11}(AsV_{10}V_2As_6O_{51})_2 \cdot 83H_2O$	7	4,5	X	35
85	Rankachite(1)	$Ca_{0.5}(V,V)(W,Fe)_2O_8(OH) \cdot 2H_2O$	7	4,5	X	6
86	Satpaevite(2)	$Al_{12}V_8O_{37} \cdot 30H_2O$	7	4,5	X	8, 17
87	Vanarsite(1)	$NaCa_{12}(AsV_{8.5}V_{3.5}As_6O_{51})_2 \cdot 78H_2O$	7	4,5	X	35
88	Vanoxite(24)	$V_6O_{13} \cdot 8H_2O$	7,8	4,5	X	14, 16, 19, 20, 29
89	Alvanite(3)	$(Zn,Ni)Al_4(VO_3)_2(OH)_{12} \cdot 2H_2O$	7	5	X	8, 17
90	Ankinovichite(2)	$NiAl_4(VO_3)_2(OH)_{12} \cdot 2H_2O$	7	5	X	8, 24
91	Ansermetite(7)	$MnV_2O_6 \cdot 4H_2O$	5	5		1, 3, 4, 10, 33
92	Aradite(1)	$BaCa_6(SiO_4)(VO_4)_3F$	3	5		76
93	Ardennite-(V)(11)	$Mn_4Al_4(AlMg)(VO_4)(SiO_4)_2(Si_3O_{10})(OH)_6$	1,5	5		45
94	Argandite(3)	$Mn_7(VO_4)_2(OH)_8$	7	5	X	1, 50
95	Averievite(1)	$Cu_5O_2(VO_4)_2 \cdot CuCl_2$	2	5		37
96	Balestraite(1)	$KLi_2VSi_4O_{12}$	3	5		48
97	Barnesite(15)	$Na_2V_6O_{16} \cdot 3H_2O$	7	5	X	3, 4, 8, 11, 13
98	Blossite(1)	$Cu_2V_2O_7$	2	5		28
99	Brackebuschite(12)	$Pb_2Mn(VO_4)_2(OH)$	7	5	X	5, 38, 43
100	Bushmakinite(2)	$Pb_2Al(PO_4)(VO_4)(OH)$	7	5	X	55
101	Calciodelrioite(3)	$Ca(VO_3)_2 \cdot 4H_2O$	7	5	X	10, 15
102	Calderónite(22)	$Pb_2Fe(VO_4)_2(OH)$	7	5	X	9, 41
103	Carnotite(1185)	$K_2(UO_2)_2(VO_4)_2 \cdot 3H_2O$	7,8	5	X	2, 4, 5, 6, 7
104	Cassedanneite(2)	$Pb_5(VO_4)_2(CrO_4)_2 \cdot H_2O$	7	5	X	59
105	Čechite(4)	$PbFeVO_4(OH)$	7,8	5	X	41
106	Cheremnykhite(1)	$Pb_3Zn_3TeO_6(VO_4)_2$	7	5	X	73
107	Chervetite(7)	$Pb_2V_2O_7$	7	5	X	5, 31

108	Clinobisvanite(38)	$BiVO_4$	7	5	X	6, 55, 58
109	Colimaite(1)	K_3VS_4	2	5		53
110	Colusite(86)	$Cu_{12}VAs_3S_{16}$	5	5		34, 36, 46, 49, 68
111	Curienite(14)	$Pb(UO_2)_2(VO_4)_2 \cdot 5H_2O$	7	5	X	5
112	Delrioite(3)	$Sr(VO_3)_2 \cdot 4H_2O$	7	5	X	16
113	Descloizite(355)	$PbZnVO_4(OH)$	7	5	X	6, 9, 12, 34, 73
114	Dickthomssenite(4)	$MgV_2O_6 \cdot 7H_2O$	7	5	X	4, 7, 10
115	Dreyerite(4)	$BiVO_4$	8	5	X	6
116	Engelhauptite(1)	$KCu_3(V_2O_7)(OH)_2Cl$	1	5		65
117	Ferribushmakinite(1)	$Pb_2Fe(PO_4)(VO_4)(OH)$	7	5	X	41
118	Fervanite(12)	$Fe_4V_4O_{16} \cdot 5H_2O$	7	5	X	2, 9, 12
119	Fianelite(2)	$Mn_2V_2O_7 \cdot 2H_2O$	5	5		33
120	Fingerite(1)	$Cu_{11}O_2(VO_4)_6$	2	5		28
121	Francevillite(38)	$Ba(UO_2)_2(VO_4)_2 \cdot 5H_2O$	7	5	X	5, 6, 18, 26
122	Franciscanite(3)	$Mn_6V(SiO_4)_2(O,OH)_6$	7	5	X	1
123	Fritzscheite(4)	$Mn(UO_2)_2(VO_4,PO_4)_2 \cdot 4H_2O$	6	5	X	83
124	Gamagarite(7)	$Ba_2Fe(VO_4)_2(OH)$	7	5	X	1, 3, 48
125	Germanocolusite(5)	$Cu_{13}VGe_3S_{16}$	5	5		34, 49
126	Gottlobite(1)	$CaMg(VO_4)(OH)$	5	5		42
127	Grigorievite(1)	$Cu_3Fe_2Al_2(VO_4)_6$	2	5		51
128	Gunterite(1)	$Na_4(H_2O)_{16}(H_2V_{10}O_{28}) \cdot 6H_2O$	7	5	X	23
129	Gurimite(1)	$Ba_3(VO_4)_2$	7	5	X	76
130	Hechtsbergite(6)	$Bi_2O(VO_4)(OH)$	5	5		6
131	Hewettite(58)	$CaV_6O_{16} \cdot 9H_2O$	7	5	X	2, 4, 7, 8, 9
132	Heyite(7)	$Pb_5Fe_2O_4(VO_4)_2$	7	5	X	9, 12, 41
133	Howardevansite(1)	$NaCuFe_2(VO_4)_3$	2	5		28
134	Huemulite(16)	$Na_4MgV_{10}O_{28} \cdot 24H_2O$	7,8	5	X	10, 15, 29, 32
135	Hughesite(3)	$Na_3Al(V_{10}O_{28}) \cdot 22H_2O$	7	5		15
136	Hummerite(21)	$KMgV_5O_{14} \cdot 8H_2O$	7	5	X	3, 9, 11, 12, 24

137	Kainotropite(1)	$Cu_4FeO_2(V_2O_7)(VO_4)$	2	5		37
138	Karpenkoite(1)	$Co_3(V_2O_7)(OH)_2 \cdot 2H_2O$	7	5	X	10
139	Kokinosite(1)	$Na_2Ca_2(V_{10}O_{28}) \cdot 24H_2O$	7	5	X	15
140	Koksharovite(1)	$CaMg_2Fe_4(VO_4)_6$	2	5		61
141	Kolovratite(2)	$(Ni,Zn)_xVO_4 \cdot nH_2O$	3,7	5	X	24
142	Kombatite(2)	$Pb_{14}O_9(VO_4)_2Cl_4$	3	5		46
143	Krettnichite(2)	$PbMn_2(VO_4)_2(OH)_2$	7	5	X	43
144	Kurumsakite(3)	$Zn_8Al_8V_2Si_5O_{35} \cdot 27H_2O$	7	5	X	8
145	Lasalite(4)	$Na_2Mg_2(V_{10}O_{28}) \cdot 20H_2O$	7	5	X	4, 7, 10
146	Leningradite(1)	$PbCu_3(VO_4)_2Cl_2$	2	5		51
147	Lyonsite(3)	$Cu_3Fe_4(VO)_6$	2	5		25, 28, 37
148	Magnesiopascoite(4)	$Ca_2MgV_{10}O_{28} \cdot 16H_2O$	7	5	X	4, 7
149	Margaritasite(2)	$Cs_2(UO_2)_2(VO_4)_2 \cdot H_2O$	2,5	5	X	54
150	Martyite(2)	$Zn_3V_2O_7(OH)_2 \cdot 2H_2O$	7	5	X	10
151	Mathesiusite(1)	$K_5(UO_2)_4(SO_4)_4(VO_5) \cdot 4H_2O$	7	5	X	85
152	Mcbirneyite(2)	$Cu_3(VO_4)_2$	2	5		28, 51
153	Medaite(5)	$Mn_6VSi_5O_{18}(OH)$	7	5	X	1, 3, 33, 45
154	Mesaite(1)	$CaMn_5(V_2O_7)_3 \cdot 12H_2O$	7	5	X	35
155	Metadelrioite(2)	$SrCa(VO_3)_2(OH)_2$	7	5	X	16
156	Metahewettite(61)	$CaV_6O_{16} \cdot 3H_2O$	7	5	X	2, 8, 10, 14, 17
157	Metamunirite(10)	$NaVO_3$	7	5	X	19, 23, 32
158	Metarossite(33)	$CaV_2O_6 \cdot 2H_2O$	7	5	X	2, 4, 7, 10, 15
159	Metatyuyamunite(122)	$Ca(UO_2)_2(VO_4)_2 \cdot 3H_2O$	7	5	X	2, 3, 6, 7, 9
160	Metavanuralite(3)	$Al(UO_2)_2(VO_4)_2(OH) \cdot 8H_2O$	7	5	X	5, 7
161	Mottramite(332)	$PbCuVO_4(OH)$	7	5	X	5, 6, 31, 34, 36
162	Mounanaite(2)	$PbFe_2(VO_4)_2(OH)_2$	7	5	X	5
163	Munirite(3)	$NaVO_3 \cdot 1.9H_2O$	7	5	X	32
mc	Nabiasite(6)	$BaMn_9(VO_4)_6(OH)_2$	5	5		1, 66
165	Namibite(25)	$Cu(BiO)_2VO_4(OH)$	1,7	5	X	6

166	Navajoite(8)	$(V,Fe)_{10}O_{24} \cdot 12H_2O$	7	5	X	2, 18
167	Nekrasovite(12)	$Cu_{13}VSn_3S_{16}$	1,5	5		36, 68
168	Palenzonaite(5)	$NaCa_2Mn_2(VO_4)_3$	3,8	5	X	1, 3, 33, 45
169	Pascoite(78)	$Ca_3V_{10}O_{28} \cdot 17H_2O$	7,8	5	X	1, 2, 4, 7, 10
170	Paseroite(1)	$PbMn(Fe,[])_2(V,Ti,[])_{18}O_{38}$	8	5	X	3
171	Pintadoite(9)	$Ca_2V_2O_7 \cdot 9H_2O$	7	5	X	11, 16, 23, 29
172	Postite(2)	$Mg(H_2O)_6Al_2(OH)_2(H_2O)_8(V_{10}O_{28}) \cdot 13H_2O$	7	5	X	4
173	Pottsite(4)	$PbBi(VO_4)(VO_3OH) \cdot 2H_2O$	7	5	X	58
174	Pseudolyonsite(1)	$Cu_3(VO_4)_2$	2	5		37
175	Pucherite(51)	$BiVO_4$	1,7	5	X	6
176	Pyrobelonite(22)	$PbMnVO_4(OH)$	3	5		1, 3, 33, 38, 43
177	Rakovanite(2)	$Na_3H_3V_{10}O_{28} \cdot 15H_2O$	7	5	X	4, 15, 23
178	Rauvite(34)	$Ca(UO_2)_2V_{10}O_{28} \cdot 16H_2O$	7	5	X	2, 13, 14, 21, 22
179	Reppiaite(2)	$Mn_5(VO_4)_2(OH)_4$	3,5	5		1, 50
180	Ronneburgite(1)	$K_2MnV_4O_{12}$	7	5	X	25, 25
181	Rossite(27)	$Ca(VO_3)_2 \cdot 4H_2O$	7	5	X	4, 7, 10, 14, 15
182	Rusakovite(1)	$(Fe,Al)_5(VO_4)_2(OH)_9 \cdot 3H_2O$	7	5	X	8, 17
183	Saneroite(3)	$Na_2(Mn,Mn)_{10}VSi_{11}O_{34}(OH)_4$	3,5,7	5		1, 3, 33
184	Santafeite(3)	$(Ca,Sr,Na)_3(Mn,Fe)_2Mn_2(VO_4)_4(OH,O)_5 \cdot 2H_2O$	7	5	X	3, 21
185	Schäferite(4)	$NaCa_2Mg_2(VO_4)_3$	3	5		39
186	Scheuchzerite(2)	$NaMn_9Si_9VO_{28}(OH)_4$	3	5		1, 33
187	Schindlerite(1)	$(NH_4)_4Na_2(V_{10}O_{28}) \cdot 10H_2O$	7,8	5	X	15
188	Schoderite(5)	$Al_2(PO_4)(VO_4) \cdot 8H_2O$	6	5	X	29
189	Schubnelite(4)	$FeVO_4 \cdot H_2O$	7	5	X	2, 5, 9, 12
190	Schumacherite(11)	$Bi_3O(VO_4)_2(OH)$	7	5	X	6
191	Sengierite(11)	$Cu_2(UO_2)_2(VO_4)_2(OH)_2 \cdot 6H_2O$	7	5	X	3, 6
192	Shcherbinaite(6)	V_2O_5	2	5	X	25, 28, 44, 51, 53
193	Sherwoodite(18)	$Ca_{4.5}AlV_2V_{12}O_{40} \cdot 28H_2O$	7,8	5	X	7, 10, 11, 13, 16
194	Starovaite(1)	$KCu_5O(VO_4)_3$	2	5		37

195	Steigerite(9)	$AlVO_4 \cdot 3H_2O$	7	5	X	2, 8, 14, 17
196	Stibiocolusite(4)	$Cu_{13}V(Sb,Sn,As)_3S_{16}$	5	5		68
197	Stoiberite(2)	$Cu_5O_2(VO_4)_2$	2	5		25, 28
198	Straczekite(4)	$(Ca,K,Ba)V_8O_{20} \cdot 3H_2O$	7	5	X	2, 18, 25
199	Strelkinite(6)	$Na_2(UO_2)_2(VO_4)_2 \cdot 6H_2O$	7	5	X	40
200	Tangeite(56)	$CaCuVO_4(OH)$	7	5	X	1, 3, 7, 21, 24
201	Tillmannsite(1)	$HgAg_3VO_4$	7	5	X	84
202	Tokyoite(6)	$Ba_2Mn(VO_4)_2(OH)$	3	5		1, 43, 48
203	Turanite(4)	$Cu_5(VO_4)_2(OH)_4$	7	5	X	9, 29
204	Turtmannite(1)	$Mn_{25}O_5(VO_4)_3(SiO_4)_3(OH)_{20}$	3	5		50
205	Tyuyamunite(637)	$Ca(UO_2)_2(VO_4)_2 \cdot 5\text{-}8H_2O$	7	5	X	2, 4, 6, 7, 9
206	Uvanite(8)	$(UO_2)_2V_6O_{17} \cdot 15H_2O$	7	5	X	2, 22
207	Vanadinite(609)	$Pb_5(VO_4)_3Cl$	7	5	X	5, 9, 12, 34, 38
208	Vanalite(2)	$NaAl_8V_{10}O_{38} \cdot 30H_2O$	7	5	X	8
209	Vanuralite(3)	$Al(UO_2)_2(VO_4)_2(OH) \cdot 11H_2O$	7	5	X	5
210	Vésigniéite(44)	$Cu_3Ba(VO_4)_2(OH)_2$	7	5	X	2, 6, 9, 12, 38
211	Volborthite(147)	$Cu_3V_2O_7(OH)_2 \cdot 2H_2O$	7	5	X	1, 3, 6, 8, 9
212	Wakefieldite-(Ce)(7)	$CeVO_4$	1,5	5		6, 38
213	Wakefieldite-(La)(2)	$LaVO_4$	1,5	5		39, 42
214	Wakefieldite-(Nd)(2)	$NdVO_4$	1,5	5		38
215	Wakefieldite-(Y)(5)	YVO_4	1,5	5		31
216	Wernerbaurite(1)	$(NH_4)_2[Ca_2(H_2O)_{14}](H_2O)_2V_{10}O_{28}$	7	5	X	15
217	Yaroshevskite(1)	$Cu_9O_2(VO_4)_4Cl_2$	2	5		37
218	Ziesite(1)	$Cu_2V_2O_7$	2	5		28
219	Ziminaite(1)	$Fe_6(VO_4)_6$	7	5	X	61

*Paragenetic Mode: 1- Intrusive igneous; 3- Metamorphic; 5- Hydrothermal; 6- Sedimentary; 7- Weathering; 8- Biologically Mediated; 9- Meteorites

Table 2. Mineral localities with the greatest diversity of V minerals, number and identity of V minerals, and their lithological settings. Listed are all localities with at least 10 different V mineral species, as well as additional localities that yielded the type specimen for all the 219 known V minerals (Table 1). The identification key to numbers for V mineral species appears in Table 1.

	Locality	# V Minerals	Lithological context (key elements)
1	Valgraveglia Mine (Gambatesa Mine), Reppia, Graveglia Valley, Ne, Genova Province, Liguria, Italy	23(12, 25, 26, 31, 37, 47, 52, 68, 91, 94, 122, 124, 153, 164, 168, 169, 176, 179, 183, 186, 200, 202, 211)	hydrothermal manganese ore deposit
2	Monument No. 2 Mine, Monument No. 2 Channel, Monument Valley, Navajo Indian Reservation, Apache Co., Arizona, USA	22(26, 38, 49, 57, 74, 75, 76, 103, 118, 131, 156, 158, 159, 166, 169, 178, 189, 195, 198, 205, 206, 210)	uranium-vanadium mine in a paleochannel composed of medium-grained, massive sandstone
3	Molinello Mine, Graveglia Valley, Ne, Genova Province, Liguria, Italy	20(10, 26, 31, 39, 43, 54, 91, 97, 124, 136, 153, 159, 168, 170, 176, 183, 184, 191, 200, 211)	hydrothermal manganese ore deposit
4	Vanadium Queen Mine, La Sal, La Sal District (Paradox Valley District), San Juan Co., Utah, USA	20(23, 26, 38, 57, 63, 75, 81, 91, 97, 103, 114, 131, 145, 148, 158, 169, 172, 177, 181, 205)	sedimentary uranium-vanadium deposit hosted in late Jurassic mudstone, sandstone
5	Mounana Mine (Mouana Mine), Franceville, Haut-Ogooué Province, Gabon	20(15, 23, 26, 38, 50, 54, 72, 75, 81, 99, 103, 107, 111, 121, 160, 161, 162, 189, 207, 209)	sedimentary uranium deposit hosted by sandstones
6	Clara Mine, Rankach valley, Oberwolfach, Wolfach, Black Forest, Baden-Württemberg, Germany	19(26, 54, 85, 103, 108, 113, 115, 121, 130, 159, 161, 165, 175, 190, 191, 205, 210, 211, 212)	barite-fluorite veins including copper, silver and lead minerals, hosted by gneisses and Triassic sandstones
7	Firefly–Pigmay Mine, La Sal Quadrangle, San Juan Co., Utah, USA	18(26, 38, 49, 72, 75, 103, 114, 131, 145, 148, 158, 159, 160, 169, 181, 193, 200, 205)	uranium-vanadium mine hosted in sandstones
8	Gold Quarry Mine (Maggie Claims; Nevada Bureau Of Mines & Geology Sample Site No. 1560; Deep West Ore Body), Maggie Creek Subdistrict, Carlin Trend, Eureka Co., Nevada, USA	17(2, 9, 74, 75, 80, 86, 89, 90, 97, 103, 131, 144, 156, 182, 195, 208, 211)	carbonate-hosted polymetallic deposit
9	Kurumsak V Deposit, Aksumbe, Karatau Range, Southern Kazakhstan Province, Kazakhstan	16(37, 64, 80, 102, 113, 118, 131, 132, 136, 159, 189, 203, 205, 207, 210, 211)	argillaceous anthraxolitic vanadiferous deposit

10	Little Eva Mine, Yellow Cat District (W. Part Of Thompsons District), Grand Co., Utah, USA	16(81, 83, 91, 101, 103, 114, 134, 138, 145, 150, 156, 158, 169, 181, 193, 205)	uranium-vanadium deposit hosted in sandstone-siltstone
11	Peanut Mine, Bull Canyon, Uravan District, Montrose Co., Colorado, USA	16(38, 49, 50, 57, 63, 75, 81, 97, 103, 131, 136, 159, 169, 171, 193, 205)	vanadium-uranium ore in sandstones
12	Carlin Gold Mine, Elko, Lynn District, Eureka Co., Nevada, USA	14(37, 64, 80, 113, 118, 131, 132, 136, 159, 189, 205, 207, 210, 211)	open pit gold mine
13	J J Mine, Paradox Valley, Uravan District, Montrose Co., Colorado, USA	14(38, 49, 57, 63, 75, 79, 81, 97, 103, 131, 159, 178, 193, 205)	vanadium mine hosted in sandstone
14	Cactus Rat Mine, Cisco, Yellow Cat District (W. Part Of Thompsons District), Grand Co., Utah, USA	12(26, 72, 76, 88, 97, 103, 131, 156, 178, 181, 195, 205)	highly organic ancient swamp deposit
15	St Jude Mine, Gypsum Valley, Slick Rock District, San Miguel Co., Colorado, USA	12(79, 83, 101, 134, 135, 139, 158, 169, 177, 181, 187, 216)	gypsum mine in sandstone
16	Jo Dandy Mine (Paradox D; Hummer; C; Blackburn; Yellow Bird No. 1; Oversight; Broker), Paradox Valley, Uravan District, Montrose Co., Colorado, USA	12(37, 38, 57, 81, 88, 97, 112, 155, 159, 171, 193, 205)	vanadium mine hosted in sandstone
17	Balasauskandyk V Deposit, Karatau Range, Southern Kazakhstan Province (Ongtüstik Qazaqstan Oblysy; Yuzhno-Kazakhstanskaya Oblast'), Kazakhstan	12(9, 74, 75, 80, 86, 89, 97, 131, 156, 182, 195, 211)	argillaceous anthraxolitic vanadiferous deposit
18	Pandora Mine, La Sal, La Sal District (Paradox Valley District), San Juan Co., Utah, USA	11(38, 72, 103, 121, 156, 158, 159, 166, 169, 181, 198)	sedimentary uranium-vanadium deposit hosted in late Jurassic mudstone, sandstone
19	Mi Vida Mine (Utex Mine), Big Indian District (Big Indian Wash - Lisbon Valley Area), San Juan Co., Utah, USA	11(26, 38, 49, 57, 75, 88, 103, 157, 159, 169, 205)	uranium-vanadium deposit hosted in calcareous sandstone
20	Parco No. 23 Mine, Parco Mine Group, Thompsons District (S. E. Thomsons), Grand Co., Utah, USA	11(26, 37, 38, 57, 75, 78, 88, 158, 159, 181, 205)	uranium-vanadium deposit hosted in sandstone-siltstone
21	Monument No. 1 Mine, Monument No. 1 Channel, Mystery Valley, Monument Valley, Navajo Indian Reservation, Navajo Co., Arizona, USA	11(26, 38, 75, 103, 131, 159, 178, 184, 200, 205, 211)	uranium-vanadium mine in a paleochannel composed of medium-grained, massive sandstone
22	Temple Mountain, San Rafael District (San Rafael Swell), Emery Co., Utah, USA	10(38, 41, 45, 56, 103, 156, 169, 178, 205, 206)	uranium deposits hosted in siliciclastic rocks
23	Sunday Mine, Slick Rock District, San Miguel Co., Colorado, USA	10(26, 38, 57, 76, 103, 128, 157, 169, 171, 177)	uranium-vanadium ore deposits in sandstone-mudstone

24	Kara-Chagyr Mountain, Fergana, Fergana Valley, Alai Range (Alay Range), Osh Oblast, Kyrgyzstan	10(26, 90, 103, 136, 141, 156, 159, 200, 211)	vanadium bearing black shales
25	Lichtenberg Absetzer Dump, Ronneburg U Deposit, Gera, Thuringia, Germany	10(63, 64, 136, 147, 180, 180, 192, 197, 198, 211)	uranium-vanadium ore deposits in sandstone-mudstone
26	Srednyaya Padma Mine, Velikaya Guba Uran-vanadium Deposit, Zaonezhie Peninsula, Lake Onega, Karelia Republic, Northern Region, Russia	9(22, 23, 26, 27, 37, 121, 158, 181, 211)	uranium-vanadium deposit hosted in sandstone
27	Ragra Mine (Minasragra), Huayllay District, Pasco Province, Pasco Department, Peru	9(26, 55, 58, 65, 72, 76, 81, 131, 169)	vanadium veins hosted in sedimentary rocks
28	Izalco Volcano, Sonsonate Department, El Salvador	9(71, 98, 120, 133, 147, 152, 192, 197, 218)	volcano rich in fumaroles and fumarolic sublimates
29	VanNavSan Claim (Van Nav Sand Claim), Fish Creek Range, Gibellini District, Eureka Co., Nevada, USA	8(74, 88, 131, 134, 156, 171, 188, 203)	carbonate-hosted polymetallic deposit
30	Pereval Marble Quarry, Slyudyanka (Sludyanka), Lake Baikal Area, Irkutskaya Oblast', Prebaikalia (Pribaikal'e), Eastern-Siberian Region, Russia	8(5, 12, 15, 17, 22, 26, 27, 33)	polymetallic deposit hosted in metamorphic rock
31	Huron River Uranium Prospect (Unnamed V Prospect; MRDS - 10171055), Huron River, Baraga Co., Michigan, USA	7(38, 107, 159, 161, 205, 211, 215)	uranium deposit in quartzite leached from surrounding rock
32	Blue Streak Mine, Bull Canyon District, Montrose Co., Colorado, USA	7(38, 73, 75, 134, 136, 157, 163)	sandstone uranium-vanadium mine
33	Fianel Mine, Ausserferrera, Ferrera Valley, Hinterrhein Valley, Grischun (Grisons; Graubünden), Switzerland	7(91, 119, 153, 168, 176, 183, 186)	iron-manganese deposit of syn-sedimentary to diagenetic origin
34	Tsumeb Mine (Tsumcorp Mine), Tsumeb, Otjikoto Region (Oshikoto), Namibia	7(2, 110, 113, 125, 161, 200, 207)	polymetallic mine hosted in dolomite
35	Packrat Mine, Gateway District, Mesa Co., Colorado, USA	7(77, 82, 84, 87, 103, 154, 205)	uranium-vanadium mine hosted in sandstone
36	Campbell Mine (Campbell Shaft), Bisbee, Warren District, Mule Mts, Cochise Co., Arizona, USA	6(23, 26, 110, 161, 167, 205)	polymetallic deposit hosted in sedimentary rocks

37	Yadovitaya Fumarole, Second Scoria Cone, Northern Breakthrough (North Breach), Great Fissure Eruption (Main Fracture), Tolbachik Volcano, Kamchatka Oblast', Far-Eastern Region, Russia	6(95, 137, 147, 174, 194, 217)	volcano rich in fumaroles and fumarolic sublimates
38	Manganese Deposit, Ilfeld, Nordhausen, Harz, Thuringia, Germany	6(99, 176, 207, 210, 212, 214)	manganese ore deposit
39	Caspar Quarry, Bellerberg Volcano, Ettringen, Mayen, Eifel, Rhineland-Palatinate, Germany	6(103, 161, 185, 200, 211, 213)	active quarry with rare minerals in basaltic rocks
40	Pick's Mine (Pick's Delta Mine; Delta Mine; Delta Uranium Mine; Hidden Splendor), Delta, San Rafael District (San Rafael Swell), Emery Co., Utah, USA	5(103, 159, 199, 205, 211)	uranium-vanadium deposit hosted in mudstone and sandstone
41	Silver Coin Mine, Valmy, Iron Point District, Humboldt Co., Nevada, USA	5(102, 105, 117, 132, 161)	vanadium bearing black shales
42	Glücksstern Mine, Gottlob Hill, Friedrichroda, Thuringian Forest, Thuringia, Germany	5(126, 200, 210, 211, 213)	barite veins, Fe-oxides ore in carbonates
43	Manganese Mine (incl. Johann Shaft; Jakob Adit), Krettnich, Wadern, Saarland, Germany	5(99, 143, 161, 176, 202)	manganese depostits in hydrothermal manganite-quartz vein
44	Vihanti Deposit (Lampinsaari Deposit; Isoaho Deposit), Vihanti, Northern Finland Region, Finland	5(5, 11, 15, 16, 192)	metamorphosed VHMS (volcanic-hosted massive sulphide) deposit.
45	Cassagna Mine, Graveglia Valley, Ne, Genova Province, Liguria, Italy	5(8, 93, 153, 168, 211)	hydrothermal manganese ore deposit
46	Kombat Mine (Klein Otavi; Asis), Kombat, Grootfontein District, Otjozondjupa Region, Namibia	4(110, 142, 161, 176)	polymetallic deposit hosted in sedimentary rocks
47	Buca Della Vena Mine, Ponte Stazzemese, Stazzema, Apuan Alps, Lucca Province, Tuscany, Italy	4(15, 38, 66, 207)	barite veins, iron-oxides ore in carbonates
48	Cerchiara Mine, Borghetto Vara, Vara Valley, La Spezia Province, Liguria, Italy	4(96, 124, 176, 202)	hydrothermal manganese ore deposit
49	Merelani Hills (Mererani), Lelatema Mts, Simanjiro District, Manyara Region, Tanzania	4(15, 20, 110, 125)	pegmatitic veins
50	Pipji Glacier, Pipjitälli, Turtmann Valley, Wallis (Valais), Switzerland	4(94, 176, 179, 204)	metamorphosed, synsedimentary, submarine-exhalative manganese-iron ores

51	Second Scoria Cone, Northern Breakthrough (North Breach), Great Fissure Eruption (Main Fracture), Tolbachik Volcano, Kamchatka Oblast', Far-Eastern Region, Russia	4(127, 146, 152, 192)	fumarole in volcano
52	Ol'khonskiye Vorota Strait (Olkhon Gate), Lake Baikal Area, Irkutskaya Oblast', Prebaikalia (Pribaikal'e), Eastern-Siberian Region, Russia	4(5, 15, 27, 36)	metamorphic rocks
53	Colima Volcano (Volcan De Fuego; Volcan De Colima), Colima Volcanic Complex, Jalisco, Mexico	4(1, 59, 109, 192)	fumarole in volcano
54	Mun. De Aldama, Chihuahua, Mexico	4(103, 149, 159, 205)	evaporites
55	Phosphate occurrence, Fumade, Castelnau-de-Brassac, Tarn, Midi-Pyrénées, France	4(100, 108, 161, 207)	black schists with phosphate nodules and quartz blocks
56	Shiti Mine, Hanbin District, Ankang Prefecture, Shaanxi Province, China	4(2, 9, 14, 26)	hydrothermal barium metallogenic belt
57	Spring Creek Mine, Wilmington, South Flinders Ranges, Flinders Ranges, South Australia, Australia	4(28, 42, 210, 211)	supergene or late-stage, low-temperature hydrothermal copper deposit
58	Linka Mine (Garnetite Mine), Spencer Hot Springs District, Lander Co., Nevada, USA	3(108, 173, 207)	tungsen ore hosted in limestones
59	Lady Anne Hopetoun Shaft (Brow And Hopeful Veins), Wanlock Dod, Leadhills, South Lanarkshire, Strathclyde, Scotland, UK	3(104, 161, 207)	coal mine
60	Yushkinite Gorge, Middle Silova-Yakha River, Pai-Khoi Range (Paikhoi; Pay Khoy), Yugorskii Peninsula, Nenetskiy Autonomous Okrug, Northern Region, Russia	3(2, 58, 70)	quartz-calcite hydrothermal veins
61	Bezymyannyi Volcano, Kamchatka Oblast', Far-Eastern Region, Russia	3(71, 140, 219)	fumarole in volcano
62	Kurase Mine, Saijo City, Ehime Prefecture, Shikoku Island, Japan	3(12, 19, 36)	metasedimentary manganese ore
63	Tanohata Mine, Tanohata-mura, Shimohei-gun, Iwate Prefecture, Tohoku Region, Honshu Island, Japan	3(26, 67, 69)	metamorphosed sedimentary manganese ore

64	Mogurazawa Mine, Kiryuu City, Gunma Prefecture, Kanto Region, Honshu Island, Japan	3(21, 26, 67)	metasedimentary manganese ore
65	Kahlenberg (Auf'm Kopp), Oberstadtfeld, Daun, Eifel, Rhineland-Palatinate, Germany	3(116, 200, 211)	scoria cone of an ancient volcano
66	Coustou Mine, Vielle Aure, Aure Valley, Hautes-Pyrénées, Midi-Pyrénées, France	3(35, 36, 164)	metamorphosed manganese ore
67	Wigwam Deposit, Revelstoke Mining Division, British Columbia, Canada	3(3, 13, 40)	lead-zinc deposit hosted in limestones
68	Chelopech Au-Cu Mine, Chelopech, Sofiya Oblast (Sofia Oblast), Bulgaria	3(110, 167, 196)	epithermal high-sulphidation gold-enargite deposit
69	Lake View Consols Mine (Lake View And Star), Golden Mile Mines, Kalgoorlie-Boulder, Kalgoorlie-Boulder Shire, Western Australia, Australia	3(23, 29, 30)	hydrothermal gold deposits
70	Phosphate Mines, Soda Springs, Caribou Co., Idaho, USA	3(61, 62, 64)	phosphatic sedimentary rocks
71	Owyhee Dam, Lake Owyhee State Park, Malheur Co., Oregon, USA	2(46, 60)	basalts and tuffs
72	First Scoria Cone (First Cinder Cone), Northern Breakthrough (North Breach), Great Fissure Eruption (Main Fracture), Tolbachik Volcano, Kamchatka Oblast', Far-Eastern Region, Russia	2(53, 192)	volcano rich in fumaroles and fumarolic sublimates
73	Delbe Orebody, Kuranakh Au Deposit, Aldan, Aldan Shield, Sakha Republic (Saha Republic; Yakutia), Eastern-Siberian Region, Russia	2(106, 113)	gold deposits in feldspar and quartz metasomatites
74	Slyudyanka (Sludyanka), Lake Baikal Area, Irkutskaya Oblast', Prebaikalia (Pribaikal'e), Eastern-Siberian Region, Russia	2(24, 39)	hydrothermal polymetallic deposit
75	Allende Meteorite (Pueblito De Allende Meteorite; Qutrixpileo Meteorite [NHM Cat.]), Pueblito De Allende, Chihuahua, Mexico	2(4, 6)	meteorite
76	Gurim Anticline, Negev, Israel	2(92, 129)	pyrometamorphic rocks

77	Gacun Mine, Maqiong, Baiyu Co., Garzê Autonomous Prefecture (Ganzi Autonomous Prefecture), Sichuan Province, China	2(18, 113)	volcanic-hosted massive sulphide (VHMS) silver-polymetallic deposit
78	Gun Claim (Gunn Claim), Wilson Lake, Itsi Mt., Watson Lake Mining District, Yukon, Canada	2(44, 67)	low temperature, late-stage quartz veins
79	Northern Breakthrough (North Breach), Great Fissure Eruption (Main Fracture), Tolbachik Volcano, Kamchatka Oblast', Far-Eastern Region, Russia	1(51)	volcano rich in fumaroles and fumarolic sublimates
80	Pereval Marble Quarry, Slyudyanka (Sludyanka), Lake Baikal Area, Irkutskaya Oblast', Prebaikalia (Pribaikal'e), Eastern-Siberian Region, Russia	1(32)	polymetallic deposit hosted in metamorphic rock (marble)
81	Byrud Emerald Mine, Minnesund, Eidsvoll (Eidsvold), Akershus, Norway	1(7)	emerald deposit in pegmatite
82	Unnamed Manganese Deposit, Shobu, Ise City, Mie Prefecture, Kinki Region, Honshu Island, Japan	1(34)	metasedimentary manganese ore
83	Schneeberg District, Erzgebirge, Saxony, Germany	1(123)	hydrothermal polymetallic deposit
84	Roua Mines (Clue de Roua), Daluis, Guillaumes, Alpes-Maritimes, Provence-Alpes-Côte d'Azur, France	1(201)	copper mine in carbonates
85	Geschieber vein, Svornost Mine (Einigkeit Mine), Jáchymov (St Joachimsthal), Jáchymov District (St Joachimsthal), Krušné Hory Mts (Erzgebirge), Karlovy Vary Region, Bohemia (Böhmen; Boehmen), Czech Republic	1(151)	quartz vein
86	Great Australia Mine, Cloncurry, Cloncurry District, Mount Isa - Cloncurry Area, Queensland, Australia	1(48)	supergene copper deposit

Table 3: Coexisting essential elements in 219 V minerals. Numbers for these coexisting elements are based on mineral species and chemical formulas in rruff.info/ima as of 15 April 2016.

Element	V total	V^{3+}	V^{4+}	V^{5+}	Element	V total	V^{3+}	V^{4+}	V^{5+}
O	211	38	51	144	B	4	4		
H	147	22	39	105	Cr	3	2		1
Ca	51	9	18	35	F	3	1	1	1
Si	37	21	8	9	Ni	3			3
Al	31	11	5	18	Ce	2	1		1
Fe	30	7	6	23	La	2	1		1
Na	29	4	7	24	Li	2		1	1
Cu	28		1	26	N	2			2
Mn	26	4	1	21	Sb	2		1	1
Ba	20	8	5	8	Sn	2			2
Pb	20			20	Tl	2		2	
Mg	17	5	2	11	Ag	1			1
S	17		10	6	Be	1	1		
K	15	1	5	13	C	1	1		
U	14			14	Co	1			1
Ti	12	10	1	2	Cs	1			1
P	10	1	5	4	Ge	1			1
As	7	1	4	6	Hg	1			1
Bi	7			7	Nd	1			1
Cl	7	1		6	Te	1			1
Zn	6			6	W	1		1	1
Sr	5		2	3	Y	1			1

Table 4: Network metrics for total V, total Cu and total terrestrial Cr minerals. Metric values for Cu and Cr mineral networks are based on Morrison et al. (2017). See text for discussion.

Networks	Edge Density	Degree centralization	Transitivity	Diameter	Mean Distance
V all	0.09350258	0.4064974	0.5030392	5	2.31707
Cu all	0.1210042	0.6841906	0.4784716	4	1.932573
Cr terrestrial	0.0528945	0.3251543	0.4400466	6	2.650876

Table 5: Estimations of undiscovered species numbers for V minerals in total and in subsets, calculated from a finite Zipf-Mandelbrot (fZM) model. Parameters of the fZM model are listed. See text for discussion.

	Total	V3+/4+	V5+	Rock-forming	Non Rock-forming	U-V deposits	Non U-V
Alpha	0.4855164	0.60341	0.4308936	0.8616267	0.4273307	0.1914736	0.8193236
A	6.30E-05	0.000333064	8.43E-05	0.001081167	7.38E-05	0.000181891	0.000201085
B	0.1490914	0.4659284	0.1778848	1.097291	0.1776986	0.120249	4.194793
P-value	0.1683843	0.6790167	0.1856256	0.4376919	0.4577854	0.4439887	0.4517901
Current Species	219	70	149	66	153	78	142
Estimated total	307	117	196	92	205	87	218
To be discovered	88	47	47	26	52	9	76
Error	30	24	21	12	19	8	34
Sample Size	5437	759	4678	492	4945	3438	1999